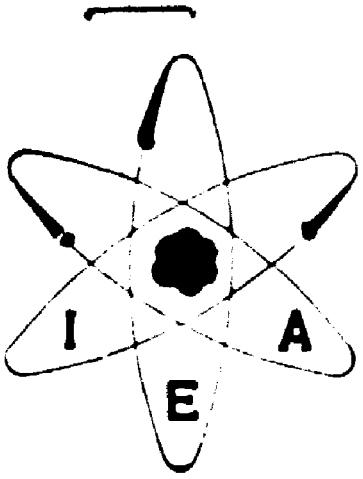

OBSERVATION OF MAGNETICALLY ANISOTROPIC DEFECTS DURING STAGE I RECOVERY IN NICKEL AFTER LOW-TEMPERATURE ELECTRON IRRADIATION

K. FORSCH, J. HEMMERICH, H. KNOLL e G. LUCKI

PUBLICAÇÃO IEA N.º 364

Novembro — 1974

INSTITUTO DE ENERGIA ATÔMICA
Caixa Postal 11049 (Pinheiros)
CIDADE UNIVERSITARIA "ARMANDO DE SALLES OLIVEIRA"
SAO PAULO — BRASIL

OBSERVATION OF MAGNETICALLY ANISOTROPIC DEFECTS DURING STAGE I RECOVERY IN NICKEL AFTER LOW-TEMPERATURE ELECTRON IRRADIATION

K. Forsch, J. Hemmerich, H. Knoll e G. Lucki

Coordenadoria de Ciência e Tecnologia de Materiais
Instituto de Energia Atômica
São Paulo - Brasil

Publicação IEA Nº 364
Novembro 1974

Instituto de Energia Atômica

Conselho Superior

Engº Roberto N. Jafet - Presidente
Prof.Dr.Emilio Mattar - Vice-Presidente
Prof.Dr.José Augusto Martins
Prof.Dr.Milton Campos
Engº Helcio Modesto da Costa

Superintendente

Rômulo Ribeiro Pieroni

OBSERVATION OF MAGNETICALLY ANISOTROPIC DEFECTS DURING STAGE I RECOVERY IN NICKEL AFTER LOW-TEMPERATURE ELECTRON IRRADIATION

K. Forsch[1], J. Hemmerich, H. Knöll[2], and G. Lucki[3]

ABSTRACT

An effort was undertaken to measure defect induced changes of magnetic anisotropy in a nickel single crystal after low temperature electron irradiation. A dynamic measuring method was used after reorienting a certain fraction of the radiation-induced defects in an external magnetic field of 5 kOe. In the temperature range of recovery stage $I_{C,D,E}$ (45 to 60 K) the crystallographic direction dependence of defect-induced anisotropy could be determined. The results show that in this temperature range the (100) split interstitial is mobile and able to reorient. The obtained data are further discussed with respect to existing information on magnetic after effect and resistivity annealing in electron irradiated nickel.

Es wurde eine Messung der defektinduzierten magnetischen in einem Nickeleinkristall nach Tieftemperatur Elektronenbestrahlung durchgeführt. Hierzu wurde eine dynamische Meßmethode nach Ausrichten eines Bruchteils der Defekte in einem externen Magnetfeld von 5 kOe angewandt. Im Temperaturbereich der Erholungsstufe $I_{C,D,E}$ (45 bis 60 K) konnte die Richtungsabhängigkeit der defektinduzierten Anisotropie bestimmt werden. Die Meßergebnisse zeigen, daß in diesem Temperaturbereich das Zwischengitteratom in der (100) Hantel Konfiguration beweglich und orientierbar ist. Die Meßergebnisse werden ferner diskutiert im Zusammenhang mit Messungen der magnetischen Nachwirkung und Widerstandserholung in elektronenbestrahltem Nickel.

1. INTRODUCTION

The interpretation of the recovery behaviour of f.c.c. metals has been the subject of a long standing controversy (see e.g. the articles[1] and[2]). In electron-irradiated Ni the radiation induced interstitials give rise to a magnetic after effect (MAE) at around 55°K (end of recovery stage I). This MAE has been observed by groups at Grenoble (Peretto et al.[3]), in Stuttgart (Lampert and Schäfer[4], Schäfer and Lampert[5]), and at Julich (knoll et al.[6]). The interpretation of this effect is controversal: Peretto et al. and Knoll and Schilling attribute it to the reorientation of interstitials during their free migration, whereas Schäfer and Lampert[5] and Kronmüller[7] attribute it to a crowdion diffusion after effect without reorientation of the interstitial. In the first case the interstitials are assumed to have the (100) split configuration and that they stabilize the Bloch wall by taking with some preference the energetically more favourable orientations within the Bloch walls. In the case of the diffusion after effect the stabilization of the Bloch walls is thought to come about by diffusion of the interstitials over long distances into or out of the bloch walls depending whether their interaction with Bloch wall magnetization is negative or positive.

A decision between both models can be made if one measures directly the alignment of interstitials in magnetically saturated samples, i.e. in samples which contain no Bloch walls.

---

1) Now at: Siemens Erlangen, Werner von Siemens Straße 50.
2) Now at Motoren- und Turbinen Union (MTU) München, 8 München 50, Dachauer Str. 665.
3) On leave from Instituto de Energia Atômica, São Paulo, Brasilien.

Because in this case no gradient of the interaction of the interstitials with the magnetization exists (like in Bloch walls) a diffusion of the defects cannot produce an inhomogeneity in the defect distribution over the sample and thus no change in the magnetization Such an experiment will be reported in the present paper It shows clearly that the interstitials have tetragonal symmetry and that they align in a magnetic field with a time constant which is about the same as that observed in the previous magnetic after effect measurements This experiment, therefore, leaves little doubt that the reorientation of (100) split interstitials is indeed responsible for the previously observed MAE in stage I of irradiated Ni

2 Method

The method for measuring small changes in magnetic anisotropy has been proposed earlier[8 9], treated in detail by Müller[10] and applied by Forsch[11 12] for investigation of anisotropy in Fe-Si alloys induced by silicon diinterstitials Basically this method works as follows: Assume a disc shaped (flat rotational ellipsoid) ferromagnetic single crystal rotating in a static external magnetic field H_a with an angular velocity ω (Fig 1) The magnetic field being perpendicular to the axis of rotation should be so strong that any domain structure is absent Under the influence of crystal anisotropy - which tries to align the magnetization in the easy direction and external field - which tries to align the magnetization in the field direction the magnetization vector in the rotating sample will perform an oscillation around the external magnetic field, thus inducing a signal in a pick-up coil

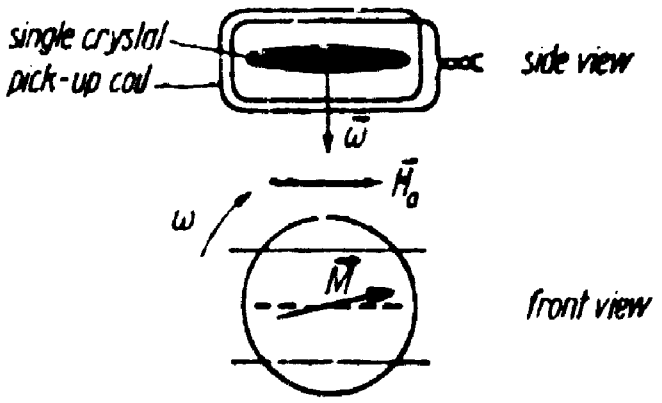

Fig. 1

Measuring principle

Fourier analysis of this signal gives direct information about anisotropy. Due to the relative smoothness of the crystal anisotropy surface a perfect (001) cut crystal induces a voltage signal in the pick up coil with only two major Fourier components (see[10–12])

$$U_{4\omega} = f \frac{\omega}{H_a} 2K_1 \tag{1}$$

$$U_{8\omega} = f \frac{\omega}{H_a} \frac{4K_1}{MH_a} \tag{2}$$

with f being a calibration factor of the apparatus, ω the rotation frequency, H_a the external field, M the magnetization, and K_1 the crystal anisotropy energy.

If we introduce anisotropic defects in the sample we should, in principle, observe an increase in anisotropy. At low defect densities this increase due to the smalleness of the signal change cannot be measured directly. Orientable defects, however, can be detected by the following method. If the sample is magnetized parallel to one of the defects anisotropy axes (at a temperature where the defects are able to reorient by thermal activation), the defects will align with some preference parallel to this direction. Since this deviation from defect equipartition has twofold symmetry, it will induce a signal with 2ω frequency:

$$U_{2\omega} = \pm f \frac{\omega}{H_a} 2K_D \tag{3}$$

K_D has been evaluated by Kronmüller[13] for a defect with tetragonal symmetry ((100) split interstitial)

$$K_D = \frac{c\epsilon_1}{2k_B T} (1 - e^{-t/\tau}), \tag{4}$$

c being defect concentration, ϵ_1 the magnetocrystalline interaction energy of the defects, τ the relaxation time for orientation, t the orientation time, and k_B the Boltzmann constant.

Applying a sensitive lock in technique the defect induced signal $U_{2\omega}$ now can easily be separated from the crystal anisotropy signal $U_{4\omega}$ which is about three orders of magnitude larger.

3 Experimental

3.1 Measuring techniques

As described in Section 2 a signal was generated in a pick up coil surrounding the sample upon rotation in a magnetic field which during all measurements was kept at 5 kOe. After passing an impedance matching transformer (PAR type AM 1) and a preamplifier bandfilter (PAR type 113) the signal was fed into the signal input of a precision lock in amplifier (PAR type HR 8). The reference signal (either with 2ω or 4ω frequency) generated exactly in phase with the sample rotation was fed into the reference input. Preirradiation tests showed the validity of (1), i.e. the proportionality of $U_{4\omega}$ with $1/H_a$ for H_a above 2.5 kOe and with ω when the sample drive was running with either 400 or 800 rpm.

The crystal anisotropy energy obtained by measuring $U_{4\omega}$ and $U_{8\omega}$ is in good agreement with that obtained by static methods (e.g.[14]) as compared in Fig. 2.

$$K_1 = \frac{1}{2} MH_a \frac{U_{8\omega}}{U_{4\omega}}$$

After irradiation the orientation anisotropy of the defects was measured by magnetizing the sample at a temperature T parallel to a main crystallographic axis during a time t resulting in a deviation from defect equipartition corresponding to (4). Rotating the sample then caused the defects to redistribute. During rotation $U_{2\omega} \sim K_D(t)$ could be recorded on a chart recorder.

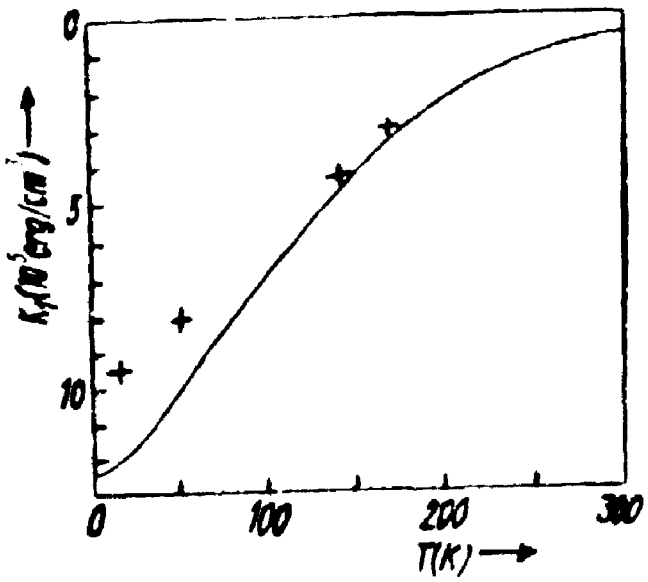

Fig 2

Crystal anisotropy energy K_1; solid line: measurements of Krause et al [14], single points: This work

3.2 Sample preparation

A 5N Ni single crystal obtained from semi elements was spark-machined to a (0001) oriented cylinder with 10 mm diameter. This cylinder was cut in slices of about 0.5 mm thickness, which were further spark and then electrochemically polished to a final thickness of 0.1 mm. These discs were soft soldered to a small copper tip on an alumina rod which could be attached to the rotation mechanism.

3.3 Cryostat

The cryostat consisted of a vacuum and liquid N_2 insulated split He reservoir containing a superconducting magnet, which could produce a field up to 5 kOe at the sample position

In the gap between the magnet coils a thermally isolated sample chamber was mounted which could be cooled by pumping helium gas from the reservoir through a cooling coil Inside this chamber an axle, fabricated from german silver, was mounted rotatable in two self-aligning composite bearings. These bearings consisted of graphite sleeves tightly fitted into stainless steel holders; mechanical dimensions and thermal coefficients of expansion of these different materials were matched to obtain temperature independent and smooth operation between liquid He and room temperature A cooper sleeve surrounding the sample could be electrically heated to control the sample temperature within ± 03 deg The temperature was measured by means of AuFe NiCr thermocouple being in thermal contact with the exchange gas near the sample During irradiation an electron beam penetrated the front window (made of 25 μ m thick stainless steel) and the sample was cooled by direct flow of liquid helium

An electronically regulated tape deck motor (with either 400 or 800 r.p.m) was connected to the sample axle by a flexible shaft

Phase and speed information for the synchronous detection of the signal was obtained by an electrooptical chooppping device mounted on the motor The correlation between the chopper and the crystallographic orientation of the sample was established by Laue graphs

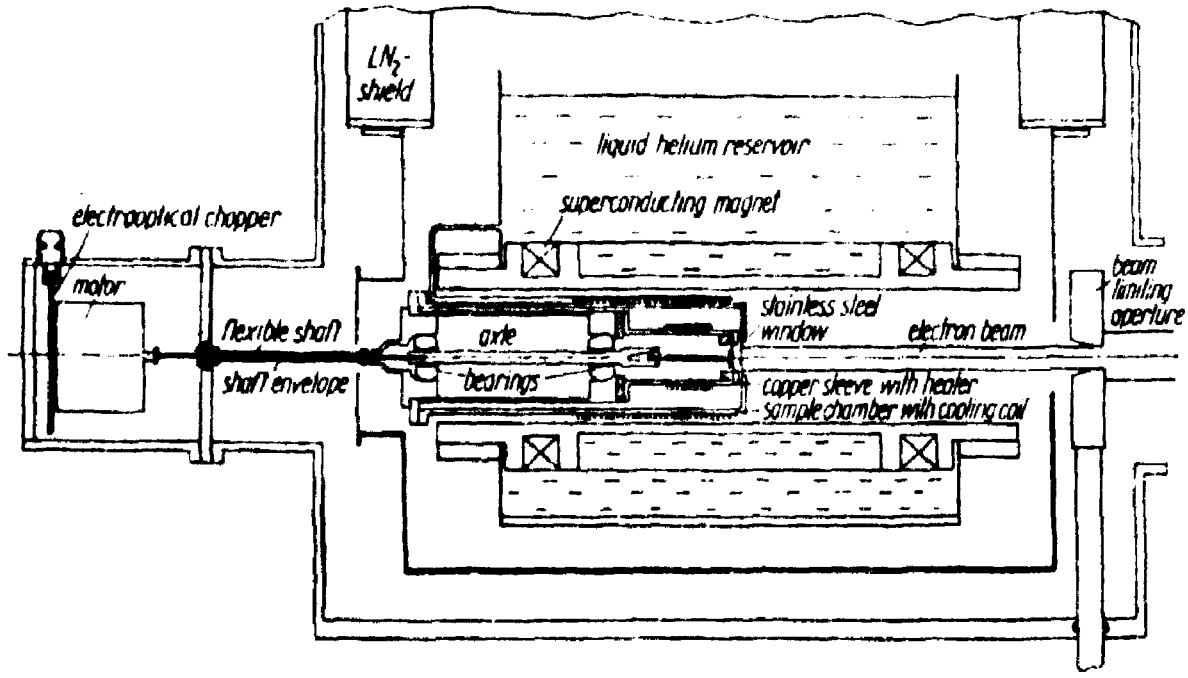

Fig. 3

Cryostat

3.4 Irradiation

The irradiation was performed at the Jülich low temperature electron irradiation facility with 3 MeV electrons the beam current density being 30 μA cm. Details about the Jülich irradiation facility have been published earlier[15]. The sample was cooled by a direct flow of liquid helium, the sample temperature remained always below 20 K. Total dose was 2.2×10^{18} electrons/cm^2 which using dose rate and resistivity measurements of Dusing[16] together with a value $\varrho_F = 6.3$ $\mu\Omega$cm/at%[17] corresponded to a defect concentration of 7.9×10^{-4}. After irradiation the cryostat was disconnected from the accelerator, the sample chamber now being kept below 20 K by indirect cooling through the cooling coil and set up for measurements.

4 Results

4.1 Defect configuration

Following the procedures outlined in Section 2 the sample was magnetized for 10 min at a constant temperature (starting at about 40 K). After magnetizing the sample was rotated at the same temperature to measure $U_{2\omega}$. In this connection it must be noted that all observed signals due to the phase shift introduced by the impedance matching transformer had a 90° phase lag with respect to the reference signal. Taking this phase shift into account we could attribute the measured signals to corresponding crystallographic directions.

After magnetizing parallel to ⟨100⟩ a maximum signal corresponding to an increase in anisotropy was found in the same direction (accounting for the above mentioned phase shift), i.e. the defect population parallel to the magnetizing and measuring direction had been increased. Magnetizing parallel to ⟨010⟩ and measuring parallel to ⟨100⟩ resulted in a signal of same amplitude but negative sign as the defect population oriented parallel to the ⟨100⟩ measuring direction had been depleted. Magnetizing the sample in ⟨110⟩ direction resulted in no signal at any phase position except for some apparatus drift or residual effect from previous ⟨100⟩ or ⟨010⟩ magnetizations.

This behaviour shows that the defects are oriented along the main crystallographic directions (⟨100⟩, ⟨010⟩, ⟨001⟩); that means the defects are ⟨100⟩ split interstitials.

4.2 Thermal behaviour

Measurements were made throughout stage $I_{C,DE}$ recovery (up to 60 K) in steps of about 2 K with the same result. Maximum signals were found after magnetizing the sample in either ⟨100⟩ or ⟨010⟩ direction. During the measurements after magnetization, i.e. during sample rotation the preferential orientation with respect to magnetic field is lost and the defect distribution returns to equipartition. During that redistribution the time law $K_D(t)$ (see equation (4)) can be determined. Detailed analysis, however, was difficult because most of the measured curves due to start up effects, long term drifts in motor speed, and temperature instability showed deviations of the pure exponential law of (4). Therefore the activation energy for defect orientation could not be determined with reasonable accuracy. A relatively good comparison, however, between magnetic after effect measurements[6,17] and anisotropy change could be performed by comparing signal amplitude changes between 40 and 600 s after start of measurements. This value is relatively free of start up effects and apparatus drifts. This

amplitude change is shown in Fig. 4, for anisotropy (solid line) and MAE (dashed line). Normalized to equal amplitudes at maximum the two curves practically coincide. The anisotropy peak is somewhat smaller than the MAE peak. The following reasons may account for that:

1. The low-temperature flank of the anisotropy change is lower because the ratio of magnetizing time (600 s) to defect relaxation time was samaller at low temperatures ($\tau \approx 2000$ s at $T = 50$ K) than at higher temperature ($\tau \approx 100$ s at $T = 56$ K). Thus at low temperatures not as many defects had time to align and the signal amplitude was smaller.

2. The high-temperature flank of the anisotropy change is also lower; this is due to annealing because during the anisotropy experiment at least twice the isochronal holding time (necessary for magnetizing and measuring) was used as compared to the MAE measurements.

coincidence of MAE with the anisotropy change clearly shows that the reorientation of ⟨100⟩ split interstitials is responsible for both effects. From the further coincidence of the MAE with recovery stage I_{D+E} (see Knoll et al.[6], Schafer and Lampert[5]) follows that during stage I in nickel ⟨100⟩ dumb-bells migrate freely by a jump mechanism combining both translation and rotation of the dumb-bell.

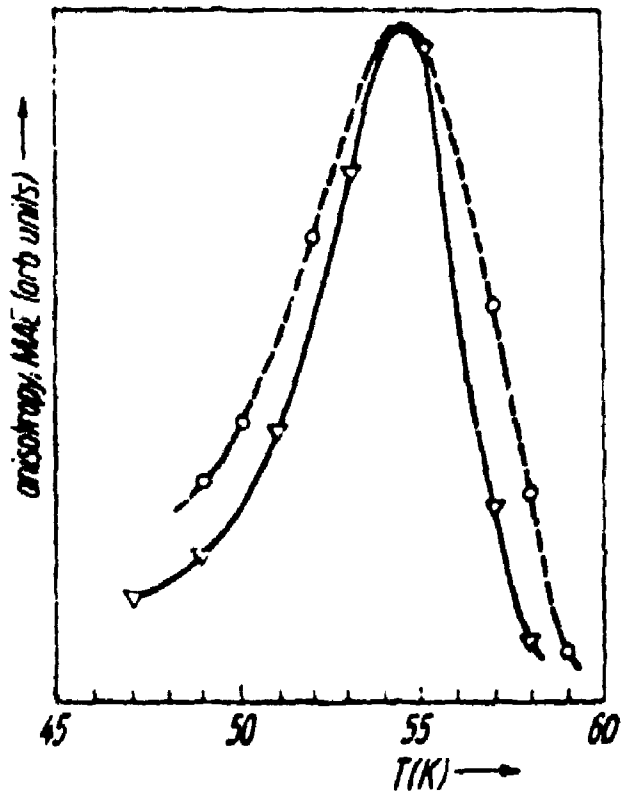

Fig. 4

Defect-induced magnetic anisotropy (solid line, ∇) and magnetic after effect (dashed line O, polycrystal) using data measured by Knoll[17].

4 3 Magnetocrystalline interaction energy

In order to compare the present information on the (100) split interstitial with other information obtainable on other defects with tetragonal symmetry we have calculated the magnetocrystalline interaction energy Using the numerical values of $U_{2\omega}$, $U_{4\omega}$, and $U_{8\omega}$ together with (1) to (4) we find a value for K_D, e g at the temperature of the maximum at 55 K.

$$K_D = 3\,5 \times 10^{-1}\, K_1 = 2\,8 \times 10^{1}\ \mathrm{erg\ cm^{-3}}$$

With the defect concentration known from irradiation data

$$c_{55K} = 4\,8 \times 10^{-4} \text{ or } 4\,3 \times 10^{19}\ \mathrm{cm^{-3}}$$

we obtain

$$\epsilon_1 = \sqrt{\frac{K_D 2kT}{c}} = 6\,2 \times 10^{-4}\ \mathrm{eV}$$

with an estimated error of ± 10% due to uncertainties in K_D and c

For other defects in irradiated Ni showing orientation MAE, Kronmüller[13] has calculated values of

$$\epsilon_1 = 3\,15 \times 10^{-4}\ \mathrm{eV}$$

for the MAE peak at 280 K,which he attributes to dumb bell reorientation, and

$$\epsilon_{eff} = 7\,4 \times 10^{-4}\ \mathrm{eV}$$

for the MAE peak at 250 K, which he attributes to divacancy reorientation.

Both effects are probably due to dumb-bell reorientation but - as taking place during recovery stage II should be attributed to rearrangement processes in interstitial clusters. Other defects with tetragonal symmetry have similar values of magnetocrystalline interaction energy, e.g., as given by Bosman and de Vries[18], for

$$\mathrm{C\ in\ \alpha\ Fe:}\ \epsilon_1 = 5\,24 \times 10^{-4}\ \mathrm{eV},$$

$$\mathrm{N\ in\ \alpha\text{-}Fe:}\ \epsilon_1 = 3\,55 \times 10^{-4}\ \mathrm{eV}$$

4. 4 Conclusion

The experimental results reported here leave no doubt that during recovery stage I the (100) split interstitial in Ni undergoes free migration combined with reorientation. This fact as a consequence very strongly supports the annealing model for f.c.c. metals proposed first by Corbett et al.[19] and later evaluated in detail by Schilling and Sonnenberg[2], who attribute the recovery taking place at the end of recovery stage I to free 3-dimensional migration of the (100) split interstitial.

Acknowledgements

The autors are especially thankful to Prof H. D Dietze and Prof W Schilling for suggesting and supporting this experiment and for many helpful discussions

RESUMO

Uma série de experiencias foi realizada no sentido de identificar os defeitos que produzem modificações na anisotropia magnetocristalina em monocristais de Níquel após irradiação com elétrons a temperatura de Hélio liquido. Foi utilizado um método de medida dinâmico, depois de reorientar uma certa fração dos defeitos de irradiação num campo magnético externo de 5 kOe. Nos estagios de recozimento $I_{C,D,E}$ (entre 45 e 60 K) a dependência da direção cristalografica da anisotropia induzida pelos defeitos foi determinada. Os resultados mostram que, nesta emplitude de temperatura, os intersticiais dissociados do tipo (100) móveis e reorientáveis. Os resultados obtidos são ainda comparados com dados existentes das medidas do efeito magnético posterior e resistividade em Níquel irradiado com elétrons.

RÉSUMÉ

Une serié d'expériences a été realizé dans le but d'indentifier les défauts responsables des madifications d'anisotropie magnétocristalline dans les monocristaux de Nikel après irradiation par électrons a la temperature à l'hélium liquide. Une méthode de mesure dynamique a été utilisée apres réorientation d'une partie des défauts d'irradiation dans un champs magnétique externe de 5 kOe. Au cours des stages de recuit $I_{C,D,E}$ (entre 45 et 60 K), a été déterminée l'influence de l'orientation cristalline sur l'anisotropie induite par les défauts. Les resultats montrent que, dans cette zone de température, les interstitiels dissociés du type (100) sont mobiles et peuvent se réorienter. Les resultats obtenus sont ensuite comparés avec ceux découlant des mesures de trainage magnétique et de résistivité dans le Nickel irradié aux électron.

REFERENCES

1 W. Schilling, G. Burger, K. Iseveck, and H. Wenzl, in: Vacancies and Interstitials in Metals, North Holland Publi. Cc, Amsterdam 1969 (p 255).
2 W. Schilling and K. Sonnenberg, J. Phys. F 3, 322 (1973)
3 - P. Peretto, J. L. Oddou, C. Minier-Cassayre, D. Dautreppe, and P. Moser, phys. stat. sol. 16, 281 (1966).
4 G. Lampert and H. E. Schäfer, phys. stat. sol. (b) 52, 475 (1972)
5 H. E. Schäfer and G. Lampert, phys. stat. sol. (b) 53, 113 (1972).
6 H. Knöll, K. Dedek, and W. Schilling, to be published in J. Phys. F 3 (1974).
7 H. Kronmüller, in: Vacancies and Interstitials in Metals, North-Holland publ. Co., Amsterdam 1969 (p. 667)
8 - E. Balthesen and H. D. Dietze, Phys. Verh. 1, 39 (1968).
9 - H. Gessinger, H. Kronmüller, and R. Bundschuh, J. Phys. E 3, 468 (1970).
10 - P. Müller, Diploma Work, Univ. Saarbrücken, 1970/71.
11 - K. Forsh, Dissertation, Univ. Saarbrücken, 1970.
12 - K. Frosch, phys. stat. sol. 42, 329 (1970).
13 - H. Kronmüller, Springer Tracts Nature Phil. 12, 253 (1968); 12, 293 (1968); 12, 311 (1968).
14 - D. Krause, B. Ludwig, and U. Patz, Z. angew. Phys. 26, 76 (1969).
15 - J. Hemmerich, W. Sassin, and W. Schilling, Z. angew. Phys. 29, 1 (1970).
16 - G. Düsing, unpublished data.
17 - H. Knoll, Ber. Kernforschungsanlage Jülich, Jül-864-FF (1972).
18 - A. J. Bosman and G. de Vries, Nederl. T. Natuurk. 27, 65 (1961).
19 - J. W. Corgett, R. B. Smith, and R. M. Walker, Phys. Rev. 114, 1452 (1959).